

# Accepted Manuscript

Structural basis of the broad substrate tolerance of the antibody 7B9-catalyzed hydrolysis of *p*-nitrobenzyl esters

Naoki Miyamoto, Miho Yoshimura, Yuji Okubo, Kayo Suzuki-Nagata, Takeshi Tsumuraya, Nobutoshi Ito, Ikuo Fujii

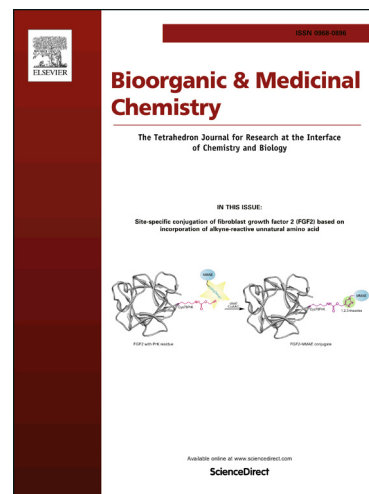
PII: S0968-0896(17)31356-1  
DOI: <http://dx.doi.org/10.1016/j.bmc.2017.07.050>  
Reference: BMC 13887

To appear in: *Bioorganic & Medicinal Chemistry*

Received Date: 5 July 2017  
Revised Date: 25 July 2017  
Accepted Date: 26 July 2017

Please cite this article as: Miyamoto, N., Yoshimura, M., Okubo, Y., Suzuki-Nagata, K., Tsumuraya, T., Ito, N., Fujii, I., Structural basis of the broad substrate tolerance of the antibody 7B9-catalyzed hydrolysis of *p*-nitrobenzyl esters, *Bioorganic & Medicinal Chemistry* (2017), doi: <http://dx.doi.org/10.1016/j.bmc.2017.07.050>

This is a PDF file of an unedited manuscript that has been accepted for publication. As a service to our customers we are providing this early version of the manuscript. The manuscript will undergo copyediting, typesetting, and review of the resulting proof before it is published in its final form. Please note that during the production process errors may be discovered which could affect the content, and all legal disclaimers that apply to the journal pertain.





## Structural basis of the broad substrate tolerance of the antibody 7B9-catalyzed hydrolysis of *p*-nitrobenzyl esters

Naoki Miyamoto <sup>a</sup>, Miho Yoshimura <sup>a</sup>, Yuji Okubo <sup>b, d</sup>, Kayo Suzuki-Nagata <sup>b, e</sup>, Takeshi Tsumuraya <sup>a</sup>, Nobutoshi Ito <sup>c</sup>, Ikuo Fujii <sup>a, \*</sup>

<sup>a</sup> Department of Biological Science, Graduate School of Science, Osaka Prefecture University, 1-1 Gakuen-cho, Naka-ku, Sakai, Osaka 599-8531, Japan.

<sup>b</sup> Biomolecular Engineering Research Institute, 6-2-3 Furuedai, Suita, Osaka 565-0874, Japan

<sup>c</sup> Medical Research Institute, Tokyo Medical and Dental University (TMDU), 1-5-45 Yushima, Bunkyo-ku, Tokyo 113-8510, Japan.

<sup>d</sup> Present address, Pharmaceutical Unit, Life Science Division, Kaneka US Innovation Center, Kaneka Americas Holding, Inc., 7979 Gateway Blvd., Suite 220, Newark, CA 94560, USA

<sup>e</sup> Present address, RIKEN Quantitative Biology Center, Laboratory for Biomolecular Structure and Dynamics, Cell Dynamic Research Core, 1-7-22 Suehiro-cho, Tsurumi-ku, Yokohama, Kanagawa 230-0045, Japan

### ARTICLE INFO

#### Article history:

Received

Received in revised form

Accepted

Available online

#### Keyword

Antibody catalyst

Hydrolysis

Substrate specificity

Catalytic mechanism

Crystal structure

Site-directed mutagenesis

### ABSTRACT

Catalytic antibody 7B9, which was elicited against *p*-nitrobenzyl phosphonate transition-state analogue (TSA) **1**, hydrolyzes a wide range of *p*-nitrobenzyl monoesters and thus shows broad substrate tolerance. To reveal the molecular basis of this substrate tolerance, the 7B9 Fab fragment complexed with *p*-nitrobenzyl ethylphosphonate **2** was crystallized and the three-dimensional structure was determined. The crystal structure showed that the strongly antigenic *p*-nitrobenzyl moiety occupied a relatively shallow antigen-combining site and therefore the alkyl moiety was located outside the pocket. These results support the observed broad substrate tolerance of 7B9 and help rationalize how 7B9 can catalyze various *p*-nitrobenzyl ester derivatives. The crystal structure also showed that three amino acid residues (Asn<sup>H33</sup>, Ser<sup>H95</sup>, and Arg<sup>L96</sup>) were placed in key positions to form hydrogen bonds with the phosphonate oxygens of the transition-state analogue. In addition, the role of these amino acid residues was examined by site-directed mutagenesis to alanine: all mutants (Asn<sup>H33</sup>Ala, Ser<sup>H95</sup>Ala, and Arg<sup>L96</sup>Ala) showed no detectable catalytic activity. Coupling the findings from our structural studies with these mutagenesis results clarified the structural basis of the observed broad substrate tolerance of antibody 7B9-catalyzed hydrolyses. Our findings provide new strategies for the generation of catalytic antibodies that accept a broad range of substrates, aiding their practical application in synthetic organic chemistry.

2009 Elsevier Ltd. All rights reserved.

### 1. Introduction

Catalytic antibodies catalyze various chemical transformations, including reactions for which no natural enzymes exist.<sup>1-4</sup> These antibodies are generated by immunization with a putative transition-state analogue (TSA), with the expectation that the induced antigen-combining site is both geometrically and electronically complementary to the transition state. Since the mammalian immune system is characterized by an almost limitless potential for providing antibody molecules for virtually any chemical compound,<sup>1,5</sup> catalytic antibodies can provide “tailor-made” catalysts for any chemical transformation if the reaction can proceed in aqueous media.<sup>1-4</sup>

Corresponding author. Tel./fax: +81-072-254-9834

E-mail address: [fujii@b.s.osakafu-u.ac.jp](mailto:fujii@b.s.osakafu-u.ac.jp)

Since antibodies possess strong binding affinity and high specificity against antigens, antibody-catalyzed reactions proceed in a highly regio- and stereo-selective manner, thereby providing a clear advantage to the development of new synthetic methods in organic syntheses. However, due to the nature of the binding of monoclonal antibodies to their substrate, the substrate specificity of an antibody-catalyzed reaction is very restricted. Consequently, the practical application of catalytic antibodies in organic synthesis requires broadening their substrate specificity.<sup>6-10</sup> We previously described the hapten design of phosphonate transition-state analogue (TSA) **1** to induce broad substrate acceptance in the antibody-catalyzed hydrolysis of *p*-nitrobenzyl esters, and the generation of antibody 7B9, which catalyzes the hydrolysis of a wide range of *p*-nitrobenzyl esters (Figure 1).<sup>11</sup> TSA **1**, composed of two different antigenic regions (a strongly antigenic *p*-nitrophenyl ring and a non-antigenic alkyl chain), was conjugated to carrier proteins to be used as an antigen.<sup>11</sup> As shown in Figure 1, antibody 7B9 catalyzes with almost identical

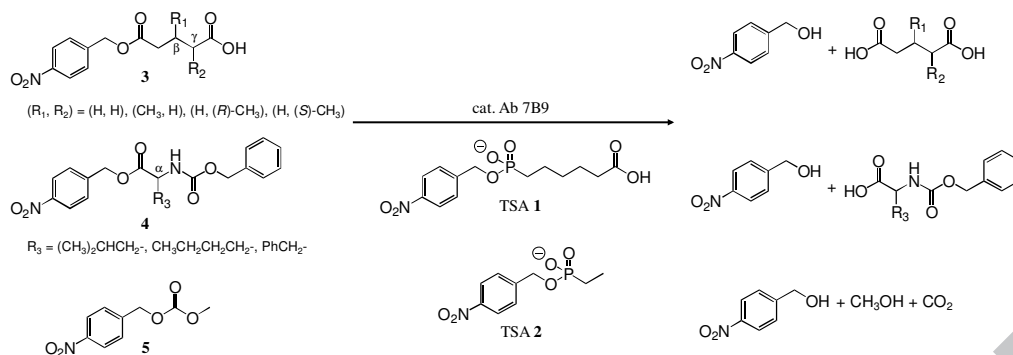


**Figure 1.** Broad substrate specificity of antibody 7B9-catalyzed hydrolysis.<sup>11</sup> Antibody 7B9 shows broad substrate specificity in catalyzing the hydrolysis of *p*-nitrobenzyl esters **3** and **4**, and *p*-nitrobenzyl methyl carbonate **5**. Antibody 7B9 was raised against TSA **1**. In the current work, TSA **2** was complexed with 7B9 and crystallized.

activity the hydrolysis of *p*-nitrobenzyl monoesters **3** of non-substituted ( $R_1, R_2 = H, H$ ),  $\beta$ -substituted ( $R_1, R_2 = CH_3, H$ ) and  $\gamma$ -substituted ( $R_1, R_2 = H, CH_3$ ) glutaric acids. In addition, 7B9 also displays substrate tolerance towards *p*-nitrobenzyl esters **4** of several amino acids (Leu, Norleu, and Phe) and *p*-nitrobenzyl methyl carbonate **5**.

In the present work, we conducted an X-ray crystal structural analysis and site-directed mutagenesis study of antibody 7B9 in order to reveal the molecular basis of its broad substrate tolerance for the hydrolysis of *p*-nitrobenzyl esters. Structural data for the 7B9 Fab fragment complexed with *p*-nitrobenzyl ethylphosphonate TSA **2** suggested that Asn<sup>H33</sup>, Ser<sup>H95</sup>, and Arg<sup>L96</sup> are catalytic residues and therefore likely stabilize the oxyanion generated in the transition state during hydrolysis. The site-directed mutagenesis studies confirmed that these amino acid residues are critical for this antibody-catalyzed hydrolysis reaction.

## 2. Results and discussion

### 2.1. Crystal structure of the catalytic antibody 7B9 Fab fragment complexed with TSA

In order to understand the mechanistic basis and the broad substrate tolerance of catalytic antibody 7B9 at a molecular level, the three-dimensional structure of the catalytic antibody complexed with TSA **2** was solved. Crystals of the complex of 7B9 Fab fragment and with **2** were grown and adopted the  $P2_1$

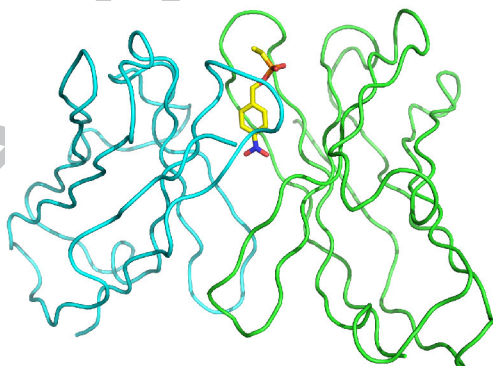


**Figure 2.** Three-dimensional structure of the complex of 7B9 (Fv) with TSA **2**. The heavy and light chains are shown as green and cyan ribbons, respectively. TSA **2** is colored according to atom type: carbon is yellow, nitrogen is blue, oxygen is red, and phosphorus is orange.

space group, with one Fab-TSA complex per asymmetric unit. The crystal structure was determined by molecular replacement and refined to an R-factor of 19.0% and a free R-factor of 25.8% at 2.2 Å resolution. As shown in Figure 2, the overall shape of the antigen-combining site is a shallow groove, rather than the deep binding pockets commonly observed in antibodies where the antigens are relatively small haptens.

A hydrophobic pocket at the bottom of the antigen-combining site is formed by the hydrophobic residues Val<sup>H37</sup>, Trp<sup>H47</sup>, Val<sup>H101</sup>, Trp<sup>H103</sup>, Leu<sup>L36</sup>, Val<sup>L89</sup>, and Phe<sup>L98</sup>. The *p*-nitrobenzyl moiety of TSA **2** is buried deep in this hydrophobic pocket (Figure 3). It is noteworthy that the three residues Val<sup>H37</sup>, Trp<sup>H47</sup>, and Phe<sup>L98</sup> were conserved in the hydrolytic antibodies CNJ206, 48G7, 17E8, 43C9, and D2.3, which were elicited against aryl-phosphonate, *p*-nitrophenyl phosphoramidate, or *p*-nitrobenzyl phosphonate transition-state analogues.<sup>11-17</sup> This similarity in the amino acid residues forming the hydrophobic pocket among hydrolytic antibodies, induced by different haptens, is consistent with the concept of “structural convergence”, in which the same key amino acid residues are utilized to conduct catalysis, even though there are large differences in the structures of the antigen-combining sites of these antibodies.<sup>16</sup>

The phosphonate moiety of **2** is located at the entrance of the 7B9 antigen-combining site and the side chains of Asn<sup>H33</sup>, Ser<sup>H95</sup>, and Arg<sup>L96</sup> are placed in key positions to interact with the

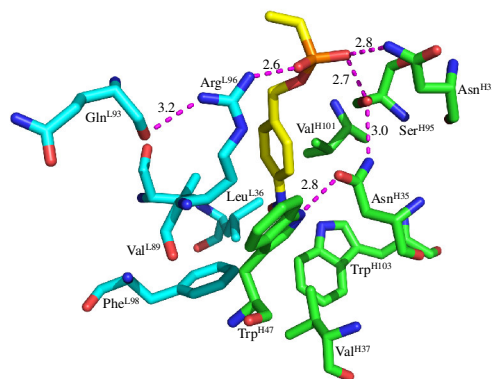


**Figure 3.** Schematic view of the key amino acid residues involved in the interaction between 7B9 and TSA **2**. The carbons of the amino acid residues in the heavy and light chains and of TSA **2** are colored in green, cyan, and yellow, respectively. Nitrogen, oxygen, and phosphorus atoms are colored in blue, red, and orange, respectively. Hydrogen bonds are shown as magenta broken lines and distances between the donor and acceptor atoms in Å are shown as black numbers.

phosphonate oxygens of **2**. The side chains of Asn<sup>H33</sup> and Ser<sup>H95</sup> form hydrogen bonds to one phosphonate oxygen, and the guanidino group of Arg<sup>L96</sup> forms a hydrogen bond to the other phosphonate oxygen (Figure 3). As described in the following section, site-directed mutagenesis of Asn<sup>H33</sup>, Ser<sup>H95</sup>, or Arg<sup>L96</sup> to alanine dramatically decreased catalytic activity, suggesting that Asn<sup>H33</sup>, Ser<sup>H95</sup>, and Arg<sup>L96</sup> stabilize the oxyanionic transition state through hydrogen bonds during antibody-catalyzed hydrolysis. Most hydrolytic enzymes utilize hydrogen bonds between the transition state and the backbone amides to stabilize the oxyanion transition state, whereas the side chain of arginine (Arg<sup>L96</sup>) plays a crucial role as an oxyanion stabilizer in several catalytic antibodies, such as 48G7, 17E8, and 43C9.<sup>18-20</sup> Antibody 7B9 also utilizes arginine at the same position (Arg<sup>L96</sup>) to stabilize the oxyanion transition state. Thus, this arginine residue is considered to be important for the catalytic hydrolysis of aryl esters and *p*-nitrobenzyl esters, also consistent with the concept of “structural convergence”.<sup>16</sup>

To understand the broad substrate tolerance of 7B9-catalyzed hydrolytic reactions, the crystal structure of 7B9 was compared with that of catalytic antibody D2.3, elicited against phosphonate transition-state analogue **6**, a hapten structurally homologous to 7B9 (Figure 4).<sup>15,16</sup> Antibody D2.3 catalyzes the hydrolysis of *N*-(*O*-*p*-nitrobenzylglutaryl)glycine **7**. However, the substrate recognition of D2.3 is different from that of 7B9.<sup>15, 21-22</sup> D2.3 recognizes not only the *p*-nitrobenzyl moiety but also the acyl part of the substrate and shows strict substrate specificity: its catalytic activity ( $k_{cat}/K_m$ ) towards *p*-nitrobenzyl acetate was dramatically decreased compared to acylated substrate **7**.<sup>15</sup> As mentioned above, although the same amino acid residues in the hydrophobic cavity at the antigen-combining site of 7B9 are also found in D2.3, the global shapes of the antigen-combining sites are totally different between 7B9 and D2.3. Antibody D2.3 possesses longer light chain CDR1 and heavy chain CDR3 loops compared to 7B9, and these long loops form a deep binding pocket in the antigen-combining site of D2.3.<sup>23</sup> In addition, two hydrogen bonds are observed between the *N*-glutarylglutamate part of hapten **6** and antibody D2.3.<sup>23</sup> In contrast, 7B9 possesses a relatively shallow binding pocket and cannot bind any moiety other than *p*-nitrobenzyl phosphonate. In the antibody-catalyzed reaction, the glutaryl moiety of the substrate would be outside the antigen-combining site and not involved in antibody recognition. Thus, 7B9 can catalyze the hydrolysis of a wide range of *p*-nitrobenzyl esters, as previously reported.<sup>11</sup>

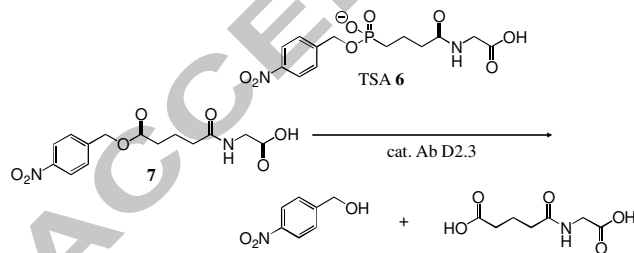


**Figure 4.** Antibody D2.3-catalyzed hydrolysis.<sup>17</sup> Antibody D2.3 was raised against TSA **6** and can catalyze the hydrolysis of substrate **7**.

Since small haptens are not immunogenic themselves, they are usually coupled to a carrier protein to provide an antigen to elicit adequate immunogenicity. Generally, simple methylene tethers are used to conjugate the transition-state analogue to the carrier protein. Little attention has been paid to the linker moiety during hapten design for the generation of catalytic antibodies. However, our results suggest the importance of the linker moiety in hapten design to generate catalytic antibodies that accept a broad range of *p*-nitrobenzyl esters.

## 2.2. Screening of mutant 7B9D from a phage-displayed library

To conduct site-directed mutagenesis studies on catalytic antibody 7B9, we attempted to use *Escherichia coli* to produce 7B9 Fab fragments using the previously described Fab expression system, pARA 7.<sup>24, 25</sup> Unfortunately, only trace amounts of 7B9 Fab fragments were produced. Since efficient production of antibody 7B9 Fab fragments in bacterial host cells was necessary to characterize the mutants, we attempted to improve the production of 7B9 Fab fragments using directed evolutionary methods. A phage-displayed library of 7B9 Fab fragments was constructed using an XL-1 Red Competent Cells for Random Mutagenesis kit: The mutations *mutS*, *mutD*, and *mutT*, which are involving in primary DNA repair pathways, were previously introduced into *E. coli* XL-1 Red strain. This triple mutant strain shows higher random mutation frequencies and rates, and is suitable for generating random mutations in the cloned gene of interest.<sup>26</sup> The phage library of 7B9 Fab fragment was screened against TSA **1** and provided several mutants with improved productivity. Of the mutants selected by biopanning, we chose the highly produced mutant 7B9D, containing the mutations Cys<sup>H44</sup>Arg, Gly<sup>L46</sup>Ser, and Glu<sup>L57</sup>Gly, for further study.

*E. coli* MC1061 carrying the expression vector pARA7 containing the 7B9D gene was grown at 37°C, then expression of the 7B9D Fab fragment gene was induced by adding arabinose. Fab fragment thus produced was partially purified by ammonium sulfate (65%) fractionation, followed by protein G affinity column chromatography, to provide purified 7B9D Fab fragment. The yield of 7B9D recombinant Fab fragment was dramatically improved (20 - 30 µg/L) compared with that of native 7B9 (< 1.0 µg/L). The dissociation constant of 7B9D for TSA **1**, and the steady-state kinetic parameters of 7B9D for the hydrolysis of *p*-nitrobenzyl methyl carbonate **5**, were determined and are summarized in Table 1. Both the 7B9 and 7B9D Fab fragments showed almost identical binding affinities against TSA **1** and catalytic activities ( $k_{cat}$ ) for the hydrolysis of carbonate **5**. It is probable that the Cys<sup>H44</sup>Arg mutation in 7B9D prevents aggregation of the protein in *E. coli*, thereby producing soluble, correctly folded Fab fragments. All induced mutations (Cys<sup>H44</sup>Arg, Gly<sup>L46</sup>Ser and Glu<sup>L57</sup>Gly) in 7B9D are remote from the antigen-combining site and thus have no effect on either binding affinity or catalytic activity. While phage-display methods are generally used to generate peptides and proteins with improved binding affinities to target molecules,<sup>27, 28</sup> our results imply that this approach can also be used to improve the yield of bacterially produced proteins.

**Table 1**

Dissociation constants of antibodies for TSA **1** and kinetic parameters of the antibody (7B9 or 7B9D)-catalyzed hydrolysis of *p*-nitrobenzyl methyl carbonate **5**.

| Antibody | $K_D$ (nM) | $k_{cat}$ (min <sup>-1</sup> ) | $K_m$ (mM) | $k_{cat}/k_{uncat}$   |
|----------|------------|--------------------------------|------------|-----------------------|
| 7B9 IgG  | 1.9±0.1    | 0.439±0.050                    | 87.0±10    | 1.9 × 10 <sup>4</sup> |
| 7B9D Fab | 1.6±0.3    | 0.231±0.037                    | 116±28     | 9.8 × 10 <sup>3</sup> |

## 2.3. Catalytic and binding activities of antibody 7B9D mutants

The crystal structure of 7B9 suggested that three residues are responsible for catalysis: Asn<sup>H33</sup>, Ser<sup>H95</sup>, and Arg<sup>L96</sup>. Therefore, the roles of these three residues in affinity and catalysis were examined by site-directed mutagenesis using the highly produced mutant 7B9D. The dissociation constants of the

mutant Fab fragments for TSA **1** (TSA) were determined by fluorescence quenching experiments.<sup>29-34</sup>

As shown in Table 2, the dissociation constants of mutants for TSA **1** were more than 100-fold lower than that of antibody 7B9D. The catalytic activities of the mutant Fab fragments for the hydrolysis of carbonate **5** were then examined using 0.9  $\mu\text{M}$  Fab fragment in 50 mM Tris-HCl, pH 8.0, at 25°C. All three mutants showed no detectable catalytic activity, strongly indicating that the side chains of Asn<sup>H33</sup>, Ser<sup>H95</sup> and Arg<sup>L96</sup> play important roles in stabilizing the oxyanion transition state in the 7B9-catalyzed hydrolysis of *p*-nitrobenzyl esters.

**Table 2**

Dissociation constants of 7B9D and its mutants for TSA **1** and their hydrolytic activities for *p*-nitrobenzyl methyl carbonate **5**.

| Antibody                    | $K_D$ (nM)    | Hydrolytic velocity ( $\mu\text{M min}^{-1}$ ) |
|-----------------------------|---------------|--|
| 7B9D                        | 1.6 $\pm$ 0.3 | 9.4 $\times 10^{-2}$                           |
| 7B9D Asn <sup>H33</sup> Ala | 167 $\pm$ 9   | 7.1 $\times 10^{-3}$                           |
| 7B9D Ser <sup>H95</sup> Ala | 125 $\pm$ 27  | 6.4 $\times 10^{-3}$                           |
| 7B9D Arg <sup>L96</sup> Ala | 283 $\pm$ 29  | 6.3 $\times 10^{-3}$                           |

<sup>a</sup>Reaction conditions: 10% DMSO/50 mM Tris HCl (pH 8.0), 25°C. The hydrolytic velocity without antibodies was 5.3  $\times 10^{-3}$   $\mu\text{M min}^{-1}$ .

### 3. Conclusions

In this work, we determined the three-dimensional structure of a catalytic antibody, 7B9, complexed with the *p*-nitrobenzyl phosphonate transition-state analogue **2**. The crystal structure shows that the overall shape of the antibody-combining site is a shallow groove. Several hydrophobic residues form a hydrophobic pocket at the bottom of the antigen-combining site and interact with the *p*-nitrobenzyl moiety of the TSA. Thus, the strongly antigenic *p*-nitrobenzyl moiety occupies a relatively shallow antigen-combining site and therefore the alkyl moiety is located outside the binding pocket. Our finding that molecular recognition occurs in a shallow pocket accounts for the broad substrate specificity of 7B9-catalyzed hydrolyses. In addition, comparison of the crystal structure of 7B9 with that of D2.3, which was elicited against a structurally similar transition-state analogue, suggests the importance of the linker moiety in hapten design. In 7B9, the alkyl chain of the linker moiety does not interact with the amino acids in the antigen-combining site, resulting in the relatively shallow binding pocket. Our structural analyses suggest that the linker moieties of haptens play an important role in achieving broad substrate tolerance. Further studies of catalytic antibodies with similar hapten designs would extend the scope of the practical application of catalytic antibodies in synthetic organic chemistry.

## 4. Materials and methods

### 4.1. Synthesis of *p*-nitrobenzyl ethylphosphonate (**2**)

A solution of diethyl ethylphosphonate (0.508 g, 3.06 mmol) in concentrated HCl (30 mL) was heated to reflux with stirring for 20 hours, then the solvent was removed *in vacuo*. To a stirred solution of the resulting residue in  $\text{CH}_2\text{Cl}_2$  (30 mL) and pyridine (10 mL) at room temperature were added *p*-nitrobenzyl alcohol (2.31 g, 15.1 mmol), DCC (3.10 g, 15.0 mmol), and <sup>1</sup>H-tetrazole (0.211 g, 3.01 mmol). After stirring for 18 hours, the reaction mixture was quenched with AcOH (1 mL) and filtered. The

filtrate was concentrated *in vacuo*, and the obtained residue was diluted with EtOAc, washed with 1 M HCl, water, sat. aqueous  $\text{NaHCO}_3$ , water, and finally brine, then dried over  $\text{Na}_2\text{SO}_4$  and concentrated *in vacuo*. The residue was purified by flash chromatography ( $\text{SiO}_2$ , EtOAc:hexane 1:1 to 1:0), to give di(*p*-nitrobenzyl) ethylphosphonate (1.07 g, 92%). To a solution of di(*p*-nitrobenzyl) ethylphosphonate (215 mg, 0.565 mmol) in  $\text{CH}_3\text{CN}$  (6 mL) was added 1 N NaOH (6 mL) at room temperature. After stirring overnight and heating at 40°C for 1 hour, the reaction mixture was acidified with 1 N HCl (6 mL) and purified by high performance liquid chromatography (HPLC) using a AM-323 (YMC Co., Ltd., Kyoto, Japan) C-18 reverse-phase column:  $\phi$  10 mm  $\times$  250 mm,  $\text{CH}_3\text{CN}/0.1\%$  aqueous TFA = 30:70, 3.0 mL/min, 254 nm, retention time 9.7 min). The  $\text{CH}_3\text{CN}$  and TFA were removed *in vacuo* and the water was removed by lyophilization to give **1** as a white solid (110 mg, 79%). <sup>1</sup>H NMR (300 MHz,  $\text{CD}_3\text{OD}$ ):  $\delta$  = 8.24 (d,  $J$  = 8.7 Hz, 2H), 7.64 (d,  $J$  = 8.7 Hz, 2H), 5.15 (d,  $J_{\text{HP}}$  = 7.9 Hz, 2H), 1.81 (dt,  $J$  = 7.7 and  $J_{\text{HP}}$  = 18.1 Hz, 2H), 1.17 (dt,  $J$  = 7.7 and  $J_{\text{HP}}$  = 20.0 Hz, 3H); <sup>13</sup>C NMR (75 MHz,  $\text{CD}_3\text{OD}$ ):  $\delta$  = 146.5, 143.3 ( $J_{\text{CP}}$  = 6.5 Hz), 126.4, 122.1, 63.6 ( $J_{\text{CP}}$  = 5.8 Hz), 17.4 ( $J_{\text{CP}}$  = 141.0 Hz), 4.3 ( $J_{\text{CP}}$  = 6.7 Hz); HRMS (FAB)  $\text{C}_9\text{H}_{11}\text{O}_5\text{NP}$ : [M-H]<sup>-</sup> calcd 244.0375, found 244.0385.

### 4.2. Production and purification of 7B9 Fab fragment from intact IgG

The antibody 7B9 was purified from ascetic fluid as previously described.<sup>35</sup> The Fab fragment was generated by papain digestion of the antibody using standard conditions.<sup>35</sup> Purified 7B9 (30 mg) was dissolved in 45 mL of 50 mM sodium phosphate (pH 7.2) containing 20 mM L-cysteine, 2 mM EDTA, and to this solution was added 5 mL of papain (100 mg/mL) dissolved in 50 mM sodium acetate, 200 mM NaCl (pH 5.0). The mixture was stirred at 25°C for 2 hours, then 5 mL of 200 mM iodoacetate solution was added to stop the enzymatic digestion. The Fab fragment was purified by mono-Q anion exchange chromatography.

### 4.3. Crystallization and data collection

The Fab fragment of 7B9 was crystallized using the hanging drop method.<sup>36</sup> The protein solution (0.5 % w/v) containing 1 mM TSA **2** was mixed in a 1:1 ratio with the reservoir buffer and then equilibrated against the reservoir buffer, which consisted of 100 mM Tris HCl (pH 8.5), 15% (w/v) PEG1000, and 5% 2-methyl-2,4-pentanediol. The crystal belonged to the  $P2_1$  space group and the asymmetric unit contained one complex of the Fab fragment and TSA **2**. Diffraction data up to 2.2 Å resolution were collected using an image plate mounted on a rotating anode at 100 K.

### 4.4. Structure determination and refinement

Structure determination and refinement were performed with the CCP4 program suite.<sup>37</sup> The structure was determined by molecular replacement using the crystal structure of another Fab fragment (PDB ID: 1kb5) as the search model.<sup>38</sup> The model was then refined using the program REFMAC<sup>39</sup> to an R-factor of 19.6% (free R-factor = 26.1%) against 17,720 reflections in the working data set between 15 and 2.2 Å.

The statistics for the data collection and structure refinement are summarized in Table 3. The coordinates and structure factors

of the Fab-inhibitor complex have been deposited in the Protein Data Bank (Entry ID: 5XQW).

**Table 3**

Data collection and refinement statistics for Fab 7B9.

|                                    |                     |
|------------------------------------|---------------------|
| Data Collection                    |                     |
| Space group                        | $P2_1$              |
| Cell dimensions                    |                     |
| $a, b, c$ (Å)                      | 44.9, 61.9, 71.0    |
| $\beta$ (deg)                      | 92.6                |
| Resolution (Å)                     | 20-2.20 (2.30-2.20) |
| $R_{\text{sym}}$                   | 0.040 (0.324)       |
| Completeness (%)                   | 98.8 (95.5)         |
| Redundancy                         | 2.6 (2.3)           |
| Refinement                         |                     |
| Resolution (Å)                     | 15-2.2              |
| No of reflections                  | 17702               |
| $R_{\text{work}}/R_{\text{free}}$  | 0.196/0.261         |
| No of atoms                        |                     |
| Protein atoms                      | 3201                |
| Ligand atoms                       | 16                  |
| Water atoms                        | 55                  |
| RMS deviations                     |                     |
| Bond length (Å)                    | 0.014               |
| Bond angles (deg)                  | 1.70                |
| Average B-factor (Å <sup>2</sup> ) | 49.4                |

\*Values in parentheses are for highest-resolution shell.

#### 4.5. Construction of the phage-displayed random library and screening of mutant antibody 7B9D molecules

Construction of the random library of 7B9 Fab fragments was carried out using an XL-1 Red Competent Cells for Random Mutagenesis kit (Agilent Technologies) according to the supplier's recommendations. The phagemid pComb3-7B9, which was constructed by ligation of the Fd and  $\kappa$  gene fragments of 7B9 into the pComb3 vector,<sup>40</sup> was transformed into *E. coli* XL-1 Red.<sup>26</sup> The transformed *E. coli* cells were cultured in LB-ampicillin medium at 37°C overnight. Phagemid DNA was extracted and transformed into *E. coli* XL-1 Blue to prepare the phage-displayed library. After four rounds of biopanning against 1-BSA, phage ELISA and DNA sequencing analysis were performed for several output clones. Then, each 7B9D Fd and  $\kappa$  gene was digested, using SpeI-XhoI for the Fd gene fragment and XbaI-SacI for the  $\kappa$  gene fragment, and ligated into the expression plasmid pARA7<sup>24</sup> to provide pARA7-7B9D.

#### 4.6. Site-directed mutation of antibody 7B9D

Asn<sup>H33</sup>, Ser<sup>H99</sup>, and Arg<sup>L96</sup> in pARA7-7B9D were separately replaced with alanine using a QuikChange Site-Directed

Mutagenesis kit (Stratagene), following the supplier's protocol. The sequences of the primers used for site-directed mutagenesis are shown below. Asn<sup>H33</sup> Ala F: 5'-GGTACTCATTCACTGACTACGCCATGAACTGGGTGAA GCAGAGC-3'; Asn<sup>H33</sup> Ala R: 5'-GCTCTGCTTCACCCAGTTCATGGCGTAGTCAGTGAATG AGTAACC-3'; Ser<sup>H95</sup> Ala F: 5'-GCAATCTATTACTGTGTAAGAGCGAATAAATACACTGG TAGCGTC-3'; Ser<sup>H95</sup> Ala R: 5'-GACGCTACCAGTGTATTTATTCGCTCTTACACAGTAATA GATTGC-3'; Arg<sup>L96</sup> Ala F: 5'-CAGTATGGCTCAGTTTCTGCGACGTCGGTGGTGGCACC -3'; Arg<sup>L96</sup> Ala R: 5'-GGTGCCACCACCGAACGTCGCAGGAACTGAGCATACT G-3'.

#### 4.7. Production of recombinant Fab fragments

The production of wild type 7B9D and mutant Fab proteins was carried out in *E. coli* MC1061.<sup>25</sup> An overnight culture (2 mL) of MC1061 harboring the pARA7 expression vector in SB medium (2% bacto tryptone, 1% bacto yeast extract, 0.5% NaCl and 0.25% K<sub>2</sub>HPO<sub>4</sub>) containing 100 µg/mL ampicillin was sub-cultured into 1 L of Circle grow medium (MP Biomedicals). The *E. coli* cells were grown to an OD<sub>600</sub> of 0.3 at 37°C, then production of the Fab fragment was induced by adding 0.2% arabinose and incubating the culture at 23°C for 3 days. The culture supernatant was salted out by adding 65% ammonium sulfate, stirring for 1 hour, then placing for 1 hour on ice. The precipitate was collected by centrifugation and was resolved in 5 mL of 10 mM sodium phosphate (pH 7.4). The suspension was dialyzed three times against 3 L of 10 mM sodium phosphate buffer (pH 7.4), centrifuged, then the supernatant was filtered and chromatographed on a Hi-Trap ProteinG HP 1 mL column (GE Healthcare). After loading at a flow rate of 0.5 mL/min, the column was washed with 20 mM sodium phosphate (pH 7.0), and the Fab fragment was eluted with 0.1 M glycine HCl (pH 2.7). The collected fractions (1 mL) were immediately neutralized by the addition of 70 µL of 1.0 M Tris-HCl (pH 9.0). The neutralized fractions containing the Fab fragment were concentrated and the buffer exchanged with 50 mM Tris-HCl (pH 8.0) using an Amicon Ultra-0.5 mL 10K centrifugal filter (Millipore).

#### 4.8. Determination of the dissociation constants for phosphonate hapten 1

Fluorescence titrations were performed on a FP-6500 fluorescence spectrometer (JASCO Corporation) equipped with a thermostated sample cell assembly through which water at 25°C was circulated. An excitation wavelength of 295 nm and an emission wavelength of 340 nm were used. After thermal equilibration, the fluorescence intensity of the antibody solution (160 nM, 200 µL in PBS) was measured at 340 nm in a micro cell. Formation of the antibody-hapten complex was followed by measuring the fluorescence quenching of the antibody solution upon addition of 2 µL aliquots of hapten 1 solution (0.05 µM, in PBS). Following each addition of hapten solution to the antibody solution, the reaction mixture was mixed by pipetting and then incubated at 25°C for 10 minutes to allow equilibration of the antibody-hapten complex. Hapten addition was continued until fluorescence quenching was saturated. Each fluorescence intensity was subtracted from the fluorescence intensity measured in the absence of hapten and this value ( $\Delta F$ ) was plotted against hapten concentration. The dissociation constant ( $K_D$ ) was

determined by fitting the curve to the following equation ( $\Delta F_{\max}$  is the value of saturated  $\Delta F$ ).<sup>30</sup>

$$[I]/\Delta F = K_D/\Delta F_{\max} + [I]/\Delta F_{\max}$$

#### 4.9. Determination of the hydrolytic activities of the 7B9D mutants

The concentrations of Fab fragments were determined by measuring their OD<sub>280</sub> using  $\epsilon = 1.4$  (0.1%, 1 cm) and molecular mass = 50,000. The catalytic activities of the antibodies (1  $\mu\text{M}$  antibody (7B9D, Asn<sup>H33</sup>Ala, Ser<sup>H99</sup>Ala, or Arg<sup>L96</sup>Ala) were examined for the hydrolysis of carbonate **5** (200  $\mu\text{M}$ ) in 50 mM Tris-HCl (pH 8.0) at 25°C. The reaction was initiated by adding 6  $\mu\text{L}$  of carbonate **5** in dimethyl sulfoxide (DMSO) to 54  $\mu\text{L}$  of the antibody solution. The hydrolysis reaction was measured by analytical HPLC using a 10  $\mu\text{L}$  injection of the reaction mixture onto a C-18 reverse-phase column from YMC, followed by elution with 0.1% aqueous trifluoroacetic acid/acetonitrile (65/35) at a flow rate of 1 mL/min and detection at 278 nm. The production of *p*-nitrobenzyl alcohol was monitored and the initial rates were determined from the linear range of the rate plot. The observed rate was corrected using the uncatalyzed rate of the hydrolysis reaction in the absence of antibody. For antibody 7B9 and 7B9D Fab fragment, the kinetic parameters  $k_{\text{cat}}$  and  $K_m$  were determined by least squares fitting to the Michaelis-Menten equation. Background rates ( $k_{\text{uncat}}$ ) were determined in the absence of antibody under otherwise identical conditions.

#### Acknowledgments

This work was supported by JSPS KAKENHI Grant Number JP20310138

#### References and notes

- Tramontano A, Janda KD, Learner RA. Catalytic antibodies. *Science*. 1986;234:1566-1570.
- Ishikawa F, Tsumuraya T, Fujii I. A Single Antibody Catalyzes Multiple Chemical Transformations upon Replacement of the Functionalized Small Nonprotein Components. *J. Am. Chem. Soc.* 2009;131:456-457.
- Ishikawa F, Uno K, Nishikawa M, Tsumuraya T, Fujii I. Antibody-catalyzed decarboxylation and aldol reactions using a primary amine molecule as a functionalized small nonprotein component. *Bioorgan. Med. Chem.* 2013;21:7011-7017.
- Ishikawa F, Shirahashi M, Hayakawa H, Yamaguchi A, Hirokawa T, Tsumuraya T, Fujii I. Site-Directed Chemical Mutations on Abzymes: Large Rate Accelerations in the Catalysis by Exchanging the Functionalized Small Nonprotein Components. *ACS Chem. Biol.* 2016;11:2803-2811.
- Tonegawa S. Somatic generation of antibody diversity. *Nature*. 1983;302:575-581.
- Iwabuchi Y, Miyashita H, Tanimura R, Kinoshita K, Kikuchi M, Fujii I. Regio- and Stereoselective Deprotection of Acylated Carbohydrates via Catalytic Antibodies. *J. Am. Chem. Soc.* 1994;116:771-772.
- Tanaka F, Kinoshita K, Tanimura R, Fujii I. Relaxing Substrate Specificity in Antibody-Catalyzed Reactions: Enantioselective Hydrolysis of N-Cbz-Amino Acid Esters. *J. Am. Chem. Soc.* 1996;118:2332-2339.
- Li T, Hilton S, Janda KD. The Potential Application of Catalytic Antibodies to Protecting Group Removal: Catalytic Antibodies with Broad Substrate Tolerance. *J. Am. Chem. Soc.* 1995;117:2123-2127.
- Hirschmann R, Smith AB, Taylor CM, Benkovic PA, Taylor SD, Yager KM, Sprengeler PA, Benkovic SJ. Peptide Synthesis Catalyzed by an Antibody Containing a Binding Site for Variable Amino Acids. *Science*. 1994;265:234-237.
- Iverson BL, Cameron KE, Jahangiri GK, Pasternak DS. Selective Cleavage of Trityl Protecting Groups Catalyzed by an Antibody. *J. Am. Chem. Soc.* 1990;112:5320-5323.
- Kurihara S, Tsumuraya T, Suzuki K, Kuroda M, Liu L, Takaoka Y, Fujii I. Antibody-Catalyzed Removal of the *p*-Nitrobenzyl Ester Protecting Group: The Molecular Basis of Broad Substrate Specificity. *Chem Eur. J.* 2000;6 (9):1656-1662.
- Zemel R, Schindler DG, Tawfik DS, Eshhar Z, Green BS. Differences in the biochemical properties of esterolytic antibodies correlate with structural diversity. *Mol. Immunol.* 1994;31:127-137.
- Lesley SA, Patten PA, Schultz PG. A genetic approach to the generation of antibodies with enhanced catalytic activities. *Proc. Natl. Acad. Sci. U.S.A.* 1993;90:1160-1165.
- Guo J, Huang W, Scanlan TS. Kinetic and mechanistic characterization of an efficient hydrolytic antibody: evidence for the formation of an acyl intermediate. *J. Am. Chem. Soc.* 1994;116:6062-6069.
- Tawfik DS, Green BS, Chap R, Sela M, Eshhar Z. catELISA: A facile general route to catalytic antibodies. *Proc. Natl. Acad. Sci. U.S.A.* 1993;90:373-377.
- Charbonnier J-B, Golinelli-Pimpaneau B, Gigant B, Tawfik DS, Chap R, Schindler DG, Kim S-H, Green BS, Eshhar Z, Knossow M. Structural Convergence in the Active Sites of a Family of Catalytic Antibodies. *Science* 1997;275:1140-1142.
- MacBeath G, Hilvert D. Hydrolytic antibodies: variations on a theme. *Chem. Biol.* 1996;3 (6):433-445.
- Wedemayer GJ, Wang LH, Patten PA, Schultz PG, Stevens RC. Crystal Structures of the Free and Liganded Form of an Esterolytic Catalytic Antibody. *J. Mol. Biol.* 1997;268:390-400.
- Wedemayer GJ, Patten PA, Wang LH, Schultz PG, Stevens RC. Structural Insights into the Evolution of an Antibody Combining Site. *Science*. 1997;276:1665-1669.
- Stewart JD, Roberts VA, Thomas NR, Getzoff ED, Benkovic SJ. Site-Directed Mutagenesis of a Catalytic Antibody: An Arginine and a Histidine Residue Play Key Roles. *Biochemistry* 1994;33:1994-2003.
- Lindner AB, Eshhar Z, Tawfik DS. Conformational Changes Affect Binding and Catalysis by Ester-hydrolysing Antibodies. *J. Mol. Biol.* 1999;285:421-430.
- Lindner AB, Kim SH, Schindler DG, Eshhar Z, Tawfik DS. Esterolytic Antibodies as Mechanistic and Structural Models of Hydrolases—A Quantitative Analysis. *J. Mol. Biol.* 2002;320:559-572.
- Gigant B, Charbonnier J-B, Eshhar Z, Green BS, Knossow M. X-ray structures of a hydrolytic antibody and of complexes elucidate catalytic pathway from substrate binding and transition state stabilization through water attack and product release. *Proc. Natl. Acad. Sci. U.S.A.* 1997;94:7857-7861.
- Cagnon C, Valverde V, Masson J-M. A new family of sugar-inducible expression vectors for *Escherichia coli*. *Protein Eng.* 1991;4 (7):843-847.
- Miyashita H, Hara T, Tanimura R, Fukuyama S, Cagnon C, Kohara A, Fujii I. Site-directed mutagenesis of active site contact residues in a hydrolytic abzyme: evidence for an essential histidine involved transition state stabilization. *J. Mol. Biol.* 1997;267:1247-1257.
- Greener A, Callahan M, Jerseth B. An efficient random mutagenesis technique using an *E. coli* mutator strain. *Mol. Biotechnol.* 1997;7:189-195.
- Smith GP. Filamentous fusion phage: novel expression vectors that display cloned antigens on the virion surface. *Science* 1985;228:1315-1317.
- Smith GP, Petrenko VA. Phage Display. *Chem. Rev.* 1997;97:391-410.
- Jolley ME, Glaudemans CPJ. The determination of binding constants for binding between carbohydrate ligands and certain proteins. *Carbohydrate Research* 1974;33:377-382.
- Ohnishi M, Yamashita T, Hiroki K. Static and Kinetic Studies by Fluorometry on the Interaction between Gluconolactone and Glucoamylase from *Rh. niveus*. *J. Biochem.* 1977;81:99-105.
- Glaudemans CPJ, Jolley ME. Methods for Measuring the Affinity between Carbohydrate Ligands and Certain Proteins. *Methods in Carbohydrate Chemistry* 1980;8:145-149.
- Friguet B, Chaffotte AF, Djavadi-Ohanian L, Goldberg ME. Measurements of the True Affinity Constant in Solution of Antigen-Antibody Complexes by Enzyme-Linked Immunosorbent Assay. *J. Immunol. Methods* 1985;77:305-319.
- Taira K, Benkovic SJ. Evaluation of the Importance of Hydrophobic Interactions in Drug Binding to Dihydrofolate Reductase. *J. Med. Chem.* 1988;31 (1):129-137.
- Hotta K, Kikuchi K, Hilvert D. Catalysis of 3-Carboxy-1,2-benzisoxazole Decarboxylation by Hydrophobic Antibody Binding Pockets. *Helv. Chim. Acta*, 2000;83:2183-2191.
- Boodhoo A, Mol CD, Lee JS, Anderson WF. Crystallization of immunoglobulin Fab fragments specific for DNA. *J. Biol. Chem.* 1988;263 (34):18578-18581.
- Foty R. A Simple Hanging Drop Cell Culture Protocol for Generation of 3D Spheroids. *J. Vis. Exp.* 2011;5:2720-2723.
- Winn MD, Ballard CC, Cowtan KD, Dodson EJ, Emsley P, Evans PR, Keegan RM, Krissinel EB, Leslie AGW, McCoy A, McNicholas SJ, Murshudov GN, Pannu NS, Potterton EA, Powell HR, Read RJ, Vagin A, Wilson KS. Overview of the CCP4 suite and current developments. *Acta. Cryst.* 2011;D67:235-242.
- Houssat D, Mazza G, Gregoire C, Piras C, Malissen B, Fontecilla-Camps JC. The three-dimensional structure of a T-cell antigen receptor V alpha V beta heterodimer reveals a novel arrangement of the V beta domain. *EMBO J.* 1997;16 (14):4205-4216.
- Murshudov GN, Skubak P, Lebedev AA, Pannu NS, Steiner RA, Nicholls RA, Winn MD, Long F, Vagin AA. REFMAC5 for the Refinement of Macromolecular Crystal Structures. *Acta. Cryst.* 2011;D67:355-367.
- Barbas CF, Kang AS, Lerner RA, Benkovic SJ. Assembly of combinatorial antibody libraries on phage surface: the gene III site. *Proc. Natl. Acad. Sci. U.S.A.* 1991;88:7978-7982.

## Graphical Abstract

To create your abstract, type over the instructions in the template box below.  
 Fonts or abstract dimensions should not be changed or altered.

**Structural basis of the broad substrate tolerance of the antibody 7B9-catalyzed hydrolysis of *p*-nitrobenzyl esters**

Leave this area blank for abstract info.

Naoki Miyamoto , Miho Yoshimura , Yuji Okubo , Kayo Suzuki-Nagata , Takeshi Tsumuraya , Nobutoshi Ito , Ikuo Fujii  
 Department of Biological Science, Graduate School of Science, Osaka Prefecture University, 1-1 Gakuen-cho, Naka-ku, Sakai, Osaka 599-8531, Japan.

